Regulatory T cells control the dynamic and site-specific T helper bias following *Salmonella* infection

Authors:

Slater L. Clay[1,2], Alberto Bravo-Blas[1,3], Daniel M. Wall[1], Megan K.L. MacLeod[1], Simon W. F. Milling[1]

Affiliations:

[1] Institute of Infection, Immunity and Inflammation, College of Medicine, Veterinary Medicine and Life Sciences, University of Glasgow, 120 University Place, Glasgow G12 8TA, United Kingdom

[2] Current affiliation: Department of Immunology and Infectious Diseases, Harvard T.H. Chan School of Public Health, 665 Huntington Avenue, Boston, MA 02115, USA

[3] Current affiliation: Institute of Cancer Sciences, University of Glasgow and Cancer Research UK Beatson Institute, Glasgow, G61 1BD, United Kingdom

Correspondence:

simon.milling@glasgow.ac.uk or sclay@hsph.harvard.edu;

Conflict of interest:

None declared.

ABSTRACT

FoxP3$^+$ regulatory T cells (Tregs) control inflammation and maintain mucosal homeostasis, but their functions during infection are less well understood. Th1, Th2 and Th17 cells can be identified by their master transcription factors (TFs) T-bet, GATA3 and RORγT; Tregs also express these TFs. While T-bet$^+$ Tregs can selectively supress Th1 cells, it is unclear whether this is true of Tregs expressing other TFs, or whether such selective suppression can alter the balance of the Th cell response. To address these questions, we used *Salmonella enterica* serotype Typhimurium (STM) to induce non-lethal colitis. Following infection, we observed an early colonic Th17 response, followed by a Th1-dominated response. The early Th17 response parallels an increase in T-bet$^+$ Tregs. Later, Th1 cells and RORγT$^+$ Tregs dominate. This reciprocal dynamic between Th cells and Tregs expressing the same TF indicates that Tregs may selectively suppress Th subsets. To test this, Treg depletion experiments were performed. These demonstrated that Tregs enable both the early colonic Th17 response and the later Th1 response. Thus, Tregs can shape the tissue CD4 T cell response in a fine-tuned manner. This highlights the potential for subpopulations of Tregs to be used in targeted therapeutic approaches.

INTRODUCTION

Salmonella enterica serovar Typhimurium (STM) infects a wide range of animals and is a common non-typhoidal Salmonella (NTS) serotype in humans. To study intestinal STM infection a streptomycin pre-treatment model has been developed, creating a niche for STM to colonise [1,2]. This facilitates consistent intestinal infection and colitis [3,4]. Because the use of virulent STM strains in susceptible mice causes high mortality, we here combine streptomycin pre-treatment with an attenuated STM strain that induces consistent non-lethal colitis. This enabled analysis of the CD4 T cell response in the colonic lamina propria and the draining lymph nodes for at least nine weeks after infection.

CD4 T helper (Th) cells drive intestinal immune responses and can express master transcription factors (TFs). T-bet, GATA3 and RORγT are used to identify Th1, Th2 and Th17 cells, respectively. CD4 T cells are critical for both clearance of STM infection and protection from re-infection [5,6]. In particular, Th1 cells are required for STM clearance and protective immunity in systemic infection [5,7–9]. In addition to Th1 cells, an early Th17 response has been identified in the intestines, where Th17 cells are important for limiting epithelial damage and systemic dissemination [10–12]. Thus, an effective immune response to STM involves both Th17 and Th1 cells. It is unclear, however, how the balance between these responses is controlled.

FoxP3$^+$ regulatory T cells (Tregs) regulate conventional T cells (Tconvs) and control the CD4 T cell response during infection [13–15]. Tregs can differentiate in the thymus (tTregs) or peripheral tissue

(pTregs). While both tTregs and pTregs are found in the intestines[16–18], their contribution to immune responses to infection is poorly characterised. In addition to FoxP3, Tregs can express Th master TFs T-bet, RORγT or GATA3 [19–22]. The role of these Treg TFs is the subject of ongoing research and there is evidence that Tregs expressing Th TFs may be able to selectively supress their respective Th subsets [21,23,24]. T-bet$^+$ Tregs can selectively target Th1 cells, but it is unclear whether Tregs expressing other TFs have similarly selective functions [21,24]. It is also unclear whether selective suppression can alter the balance of Th cell responses during infection.

To investigate the role of Treg populations in controlling the CD4 T cell response, we employed a model of STM colitis using streptomycin pre-treatment and an attenuated bacterial strain. Characterisation of Tconvs and Tregs over time, highlighted a dynamic colonic T cell response dominated initially by Th17 cells and followed by a sustained Th1 response. Interestingly, in the colon, we identified a reciprocal dynamic between Tconvs and Tregs expressing the same TFs. This reciprocity indicated that subpopulations of Tregs may selectively suppress Th subsets. Treg depletion experiments were therefore carried out using “DEpletion of REGulatory T cell” (DEREG) mice[25]. Results from these experiments show that Tregs are necessary for the early Th17 response and also contribute to the later Th1 bias. Thus, Tregs not only inhibit CD4 T cells, but can shape the T cell response in a fine-tuned, tissue-specific manner.

RESULTS

Salmonella infection with STM BRD509-2W1S causes non-lethal colitis with transient weight loss and increased numbers of total and antigen-specific CD4 T cells

To investigate the CD4 T cell response to STM in the intestines, attenuated STM strain BRD509-2W1S was orally administered to C57BL/6 mice 24 hrs following streptomycin treatment. Infection caused non-lethal colitis and allowed identification of STM-specific T cells. Representative images of large intestines, including the caecum and colon are shown from infected (top) and uninfected (bottom) animals 6 days post-infection (p.i.) (Fig. 1a). Infected tissues show colonic shortening, oedema, empty and shrivelled caeca and an enlarged caecal patch (Fig. 1a, inset). Despite physical signs of colitis, STM-infected mice lost <5% of initial weight, which recovered to levels of mock (PBS)-infected controls by 14 days p.i. (Fig. 1b). To assess bacterial dissemination, intestinal and lymphoid tissues were processed and plated. At day 6 p.i. STM CFUs were recovered from the colon, mesenteric lymph nodes (MLN), Peyer’s patches (PP) and small intestine (SI); significantly more CFUs were recovered from the colon and MLN than the SI (Fig. 1c).

Next, changes in total cell numbers, CD4 T cells and FoxP3$^+$ Tregs were enumerated in the colonic lamina propria (LP) (Fig. 1d) and MLN (Fig. 1e) at day 6, 30 and 60 days p.i. In the colon there was a significant increase in the number of total cells, CD4 T cells and Tregs at day 6 p.i., and total cell

numbers remained elevated until 60 days p.i. (Fig. 1d). The number of total MLN cells also increased 6 days p.i., but this increase was resolved by day 30 p.i. Unlike in the colon, there was no significant increase in the number of MLN CD4 T cells or Tregs (Fig. 1e).

Infection with STM strain BRD509-2W1S allows identification of STM-specific T cells with 2W1S:I-A^b tetramers (Figure S1). In the colon and caecum, 2W1S-specific cells comprise 5-10% of total CD4 T cells (Fig. 1f, Figure S2), but are less frequent in lymphoid tissues including MLNs (Fig. 1g, Figure S2). Tracking 2W1S-specific CD4 T cells over time showed these cells were detectable until at least 90 days p.i. (Fig. 1f, g).

Fig. 1

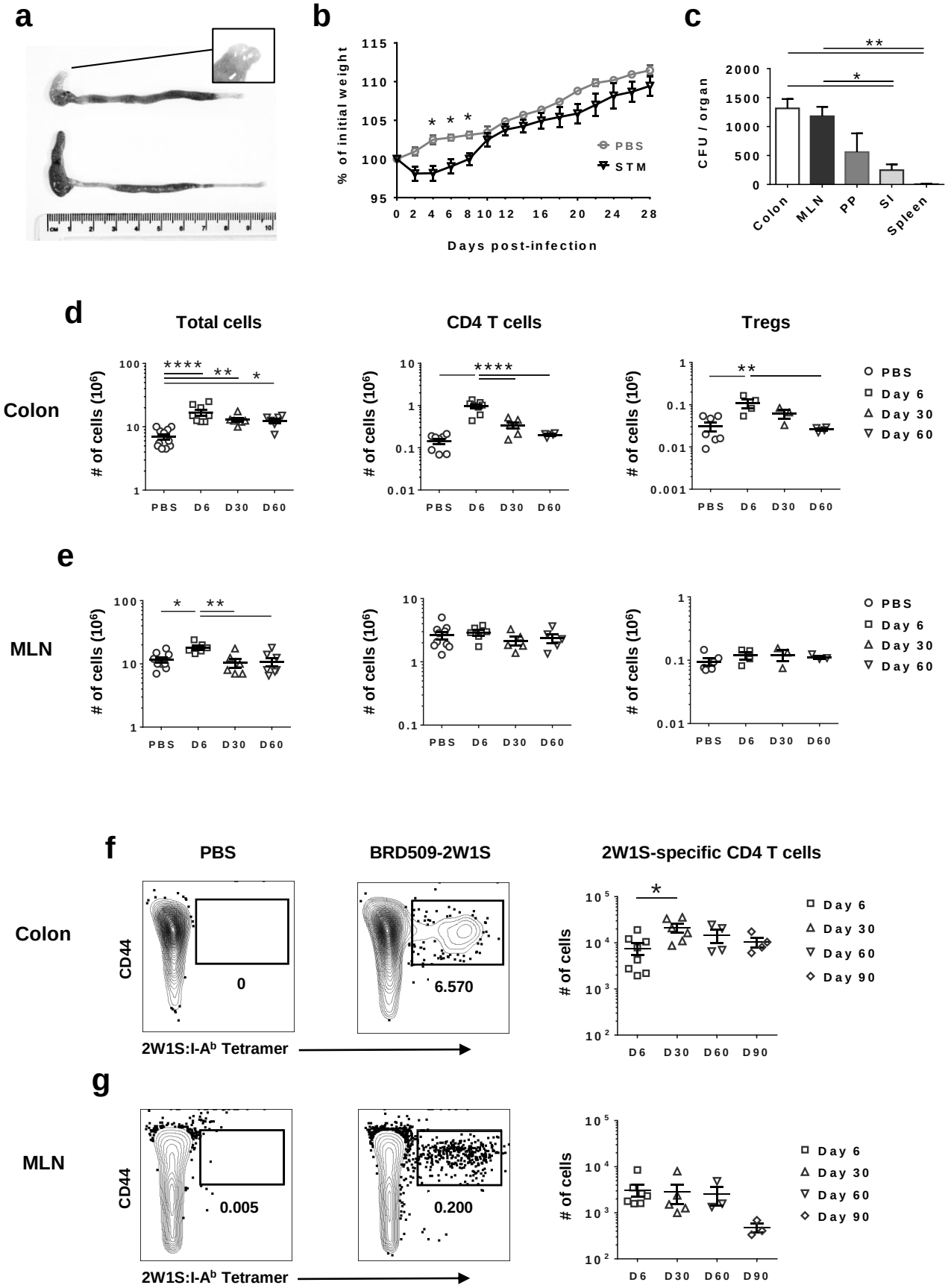
a
b
% of initial weight
Days post-infection
PBS
STM
c
CFU / organ
Colon
MLN
PP
SI
Spleen
d
Total cells
CD4 T cells
Tregs
Colon
# of cells (10^6)
PBS
D6
D30
D60
Day 6
Day 30
Day 60
e
MLN
f
PBS
BRD509-2W1S
2W1S-specific CD4 T cells
Colon
CD44
0
6.570
2W1S:I-A^b Tetramer
# of cells
Day 90
g
MLN
0.005
0.200

Fig. 1 Oral administration of STM strain BRD509-2W1S induces non-lethal intestinal infection, colitis and STM-specific CD4 T cells in the colon and MLN. **a** Representative images of colon and caeca from infected (top) and uninfected (bottom) mice, 6 days p.i. Inset shows the tip of infected caecum with enlarged caecal patch. **b** Change in initial weight is plotted following infection with BRD509-2W1S or mock infection with PBS. **c** STM CFUs recovered from five tissues 6 days p.i. are plotted. **d** The number of total colonic cells, CD4 T cells and Tregs are plotted from PBS (mock)-infected and STM-infected mice at day 6, 30 and 60 p.i. Total cells are plotted as enumerated from single cell suspension by haemocytometer. Colonic CD4 T cells were identified by flow cytometry as live, single $CD45^+$, $CD3^+$, $Dump^-$ (MHCII, B220, CD8, CD64) $CD4^+$ cells and Tregs were identified as $FoxP3^+$ CD4 T cells. **e** Total MLN cells, CD4 T cells and Tregs were identified and plotted at the same timepoints as above. **f** Representative plots show the proportion of CD4 T cells that are labelled with 2WIS:1-A^b tetramers in mock-infected (left) and BRD509-2W1S-infected samples (middle). The number of 2W1S-specific colonic CD4 T cells are plotted (right) at day 6, 30, 60 and 90 p.i. **g** Representative plots and charts of 2W1S-specific CD4 T cells in the MLN are displayed as above. Weight charts (**b**) show data from two independent experiments (*n*=3-5) and CFU data (**c**) is from one experiment (*n*=3). Data points (**d-g**) represent individual animals from 2 independent experiments (*n*=3-11). In all charts, mean ± standard error of the mean (SEM) are plotted. Statistical significance between weights at specific time points are calculated by multiple Student's t tests. Statistical difference between all other groups are calculated by one-way ANOVA with Tukey's test. ns, not significant; **p*<.05; ***p*<.01; ****p*<.001; *****p*<.0001.

The MLN CD4 T cell response to Salmonella is constrained to colon-draining MLNs

The higher bacterial burden and number of 2W1S-specific T cells observed in the large intestine compared to the SI (Fig. 1c, Figure S2), led to the hypothesis that the MLN CD4 T cell response was focused in the colon and caecum draining MLNs (cMLNs). This hypothesis is consistent with previous work showing that different intestinal sites drain to specific MLNs [26,27] (Figure S3a). With the aim of improving sensitivity of detecting STM responses in the MLNs, a comparison of CD4 T cells in the cMLN and sMLN was conducted following STM infection. Results show that cMLNs but not sMLNs contain an increased number of total cells, CD4 T cells, $CXCR3^+$ CD4 T cells and 2W1S-specific T cells (Figure S3b, c). Together, these data show that the CD4 T cell response to STM in the MLN is restricted to the colon and caecum-draining lymph nodes.

The CD4 T cell response to STM comprises an early colonic Th17 response followed by a sustained Th1 response

To characterise the CD4 T cell response we analysed activated conventional T cells (Tconvs) expressing master transcription factors (TFs). Tconvs were identified as CD4 T cells (gated as described in Fig. 1d) that are $CD44^{hi}$ and $FoxP3^-$ (Fig. 2a, left). Tconvs were characterised by expression of T-bet, RORγT and GATA3 to identify Th1, Th17 and Th2 cells respectively[28]. We initially examined the 2W1S-specific T cell response, and observed that 2W1S-specific T cells homogenously display a Th1 phenotype at all time points following infection (Figure S4), consistent with previous reports[29,30]. In contrast, the total CD4 T cell response following STM infection comprises heterogenous and dynamic populations of Th1 cells, Th17 cells, and Tregs. To assess changes in Th subsets and Tregs following infection, the bulk CD4 T cell pool was therefore characterised in the subsequent experiments.

The number and proportion of cMLN (Fig. 2b) and colonic LP (Fig. 2c) CD44^{hi} Tconvs are plotted from mock (PBS)-infected mice and STM-infected mice harvested at 6, 30 or 60 days p.i. In the cMLN, there are increased numbers (Fig. 2b, left) and proportions (Fig. 2b, right) of Tconvs that are Th1, Th17 and T-bet^{+}RORγT^{+} cells at 6 days p.i. Numbers of all subsets except Th1 cells return to baseline levels by day 30 p.i., while Th1 cells remain increased until 60 days p.i. In the colonic LP there is an increased number of Tconvs expressing T-bet (Th1), RORγT (Th17) or T-bet and RORγT 6 days p.i (Fig. 2c, left). While Th1, Th17, and T-bet^{+}RORγT^{+} cells increase in number, the increase in Th17 cells is greater, leading to an increased proportion of Th17 cells and a decreased proportion of Th1 and Th2 cells at d6 (Fig. 2c, right). This Th17 bias at 6 days p.i. is transient however, and by day 30 p.i. a strong Th1 bias is observed. Cytokine staining of PMA Ionomycin-stimulated cells shows that T-bet^{+} Tconvs produce predominantly IFNγ, and RORγT^{+} Tconvs produce IL17A, which supports the characterisation of these cells as Th1 and Th17 (Figure S5). In summary, there is an initial colonic Th17 response which shifts to a long-lasting Th1 response. This dynamic CD4 T cell response is observed in the colonic mucosa but not in the cMLN.

Fig. 2

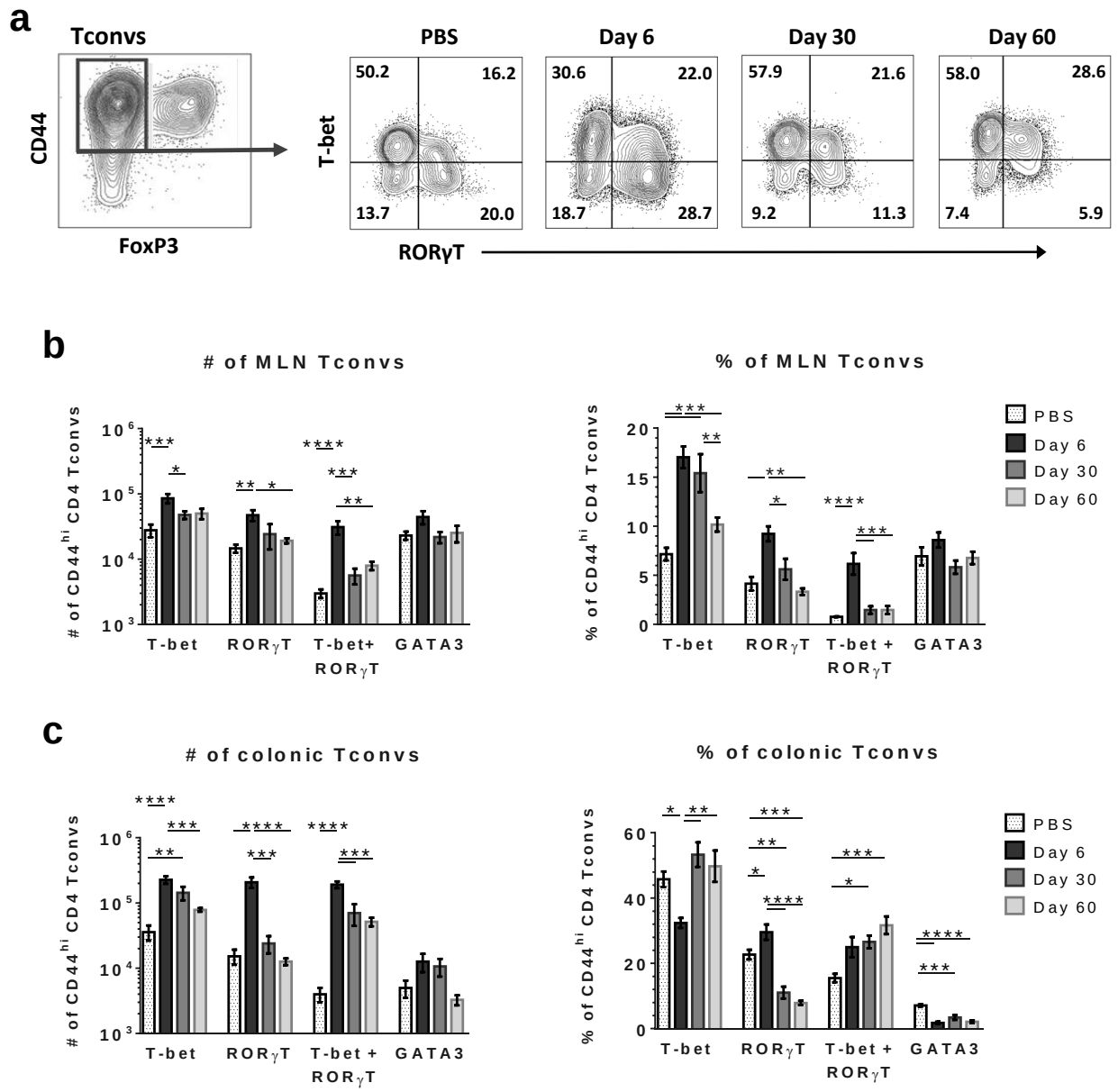

Fig. 2 At day 6 p.i. the proportion of Tbet^{+} colonic Tconvs decreases while the proportion of RORγT^{+} Tconvs increases. **a** Representative plots of colonic Tconvs (CD44^{hi} FoxP3^{-} CD4 T cells, gated left) stained for T-bet and RORγT, following STM or mock (PBS) infection. **b** TF expression by MLN Tconvs, shown as absolute numbers (left) or proportions of Tconvs (right). **c** TF expression by colonic Tconvs, shown as absolute numbers (left) or proportions of Tconvs (right). Means ± SEM are plotted (*n*=3-6 animals/group) and are representative of three independent experiments. Statistical significance calculated by one-way ANOVA with Tukey's test for each TF. ns, not significant; **p*<.05; ***p*<.01; ****p*<.001; *****p*<.0001.

Reciprocal dynamics between colonic Tconvs and Tregs expressing the same TFs

Following characterisation of the Tconv response, FoxP3^{+} Tregs were assessed for expression of Th master TFs T-bet, RORγT and GATA3 (Fig. 3a, b). The number and proportion of colon Tregs expressing these TFs were plotted from mock (PBS)-infected mice or STM-infected mice harvested

at 6, 30 or 60 days p.i. (Fig. 3b). There was an increased number of Tregs that were T-bet$^+$ and T-bet$^+$RORγT$^+$ at 6 days p.i., but no increase of RORγT$^+$ or GATA3$^+$ Tregs. The changes in absolute number correspond with an increased proportion of Tregs that were T-bet$^+$ and a reduced proportion of RORγT$^+$ Tregs at day 6 p.i. While these proportional changes are partially resolved by day 60 p.i., the percentage of Tregs that are T-bet$^+$ remain elevated while the proportion of RORγT$^+$ Tregs remain lower than mock-infected controls (Fig. 3b, right).

Comparing the proportion of colonic Tconvs and Tregs expressing T-bet or RORγT reveals a reciprocal dynamic between populations expressing the same TF. The early decrease in the proportion of colonic Th1 cells (Fig. 2c, right) occurs concurrently with an increased proportion of T-bet$^+$ Tregs (Fig. 3b, right). Conversely, the transient increase in the proportion of Th17 cells corresponds with transient decrease in the proportion of Tregs that are RORγT$^+$.

To further investigate this reciprocity, a more detailed time-course was carried out during the first 30 days p.i. In Fig. 3c-d, the proportions of Tregs that are T-bet$^+$ or RORγT$^+$ (black lines) are overlaid with the proportion of Tconvs (grey lines) that express the same TFs. These plots highlight a reciprocal dynamic between Tconvs and Tregs expressing T-bet or RORγT in the colon, but not the cMLN. Furthermore, these data show that day 6 p.i. is the peak of the colonic Th17 response and a Th1 bias is re-established by day 11 p.i (Fig. 3c). In summary, the early Th17 response in the colon coincides with an increased proportion of T-bet$^+$ Tregs, and the later Th1 bias coincides with an increased proportion of RORγT$^+$ Tregs. This dynamic is consistent with the hypothesis that Th1 cells are selectively suppressed by T-bet$^+$ Tregs and Th17 cells are selectively targeted by RORγT$^+$ Tregs.

Fig. 3

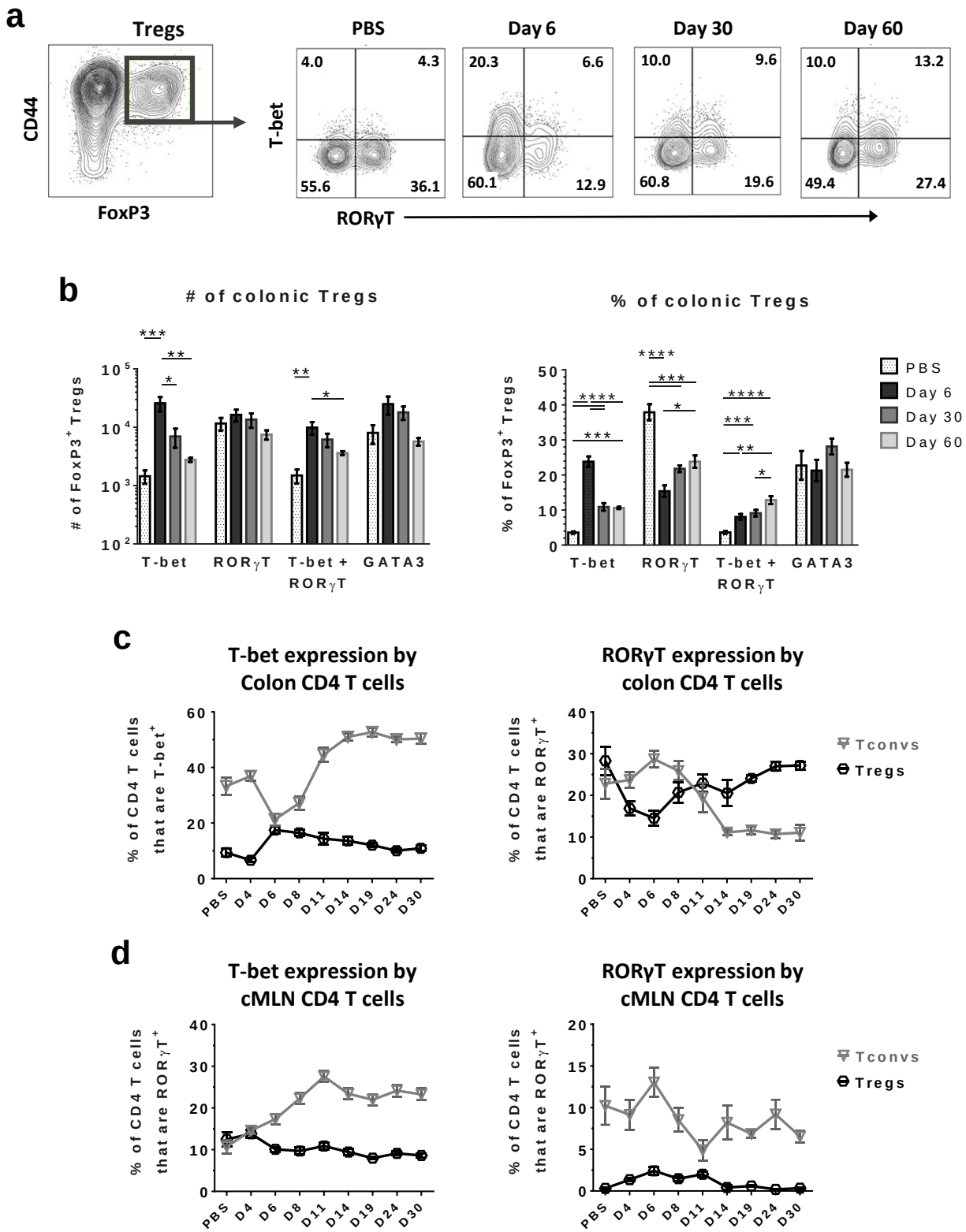
a
Tregs
CD44
FoxP3
PBS
Day 6
Day 30
Day 60
T-bet
RORγT
4.0
4.3
55.6
36.1
20.3
6.6
60.1
12.9
10.0
9.6
60.8
19.6
10.0
13.2
49.4
27.4
b
# of colonic Tregs
% of colonic Tregs
# of FoxP3+ Tregs
% of FoxP3+ Tregs
T-bet
RORγT
T-bet + RORγT
GATA3
PBS
Day 6
Day 30
Day 60
c
T-bet expression by Colon CD4 T cells
RORγT expression by colon CD4 T cells
% of CD4 T cells that are T-bet+
% of CD4 T cells that are RORγT+
Tconvs
Tregs
PBS
D4
D6
D8
D11
D14
D19
D24
D30
d
T-bet expression by cMLN CD4 T cells
RORγT expression by cMLN CD4 T cells

Fig. 3 Transcription factor expression in FoxP3$^+$ Tregs reveals reciprocity between Tconvs and Tregs expressing T-bet or RORγT in the colon but not the cMLNs. **a** Representative plots of colon Tregs (FoxP3$^+$ CD4 T cells, gated left) stained for T-bet and RORγT following mock (PBS) or STM infection. **b** Expression of TFs by colonic Tregs are shown as absolute numbers (left) or proportions of Tregs (right). **c** Line charts show changes in in the proportion of colon Tregs and Tconvs expressing T-bet (left) or RORγT (right) during the first 30 days p.i. **d** The expression of T-bet or RORγT by cMLN Tconvs and Tregs are shown. Means ± SEM are plotted (*n*=3-6 animals/group) and are representative of three independent experiments (**b**). Statistical significance calculated by one-way ANOVA with Tukey's test for each TF. ns, not significant; **p*<.05; ***p*<.01; ****p*<.001; *****p*<.0001.

Helios^{hi} Tregs include T-bet$^+$ and GATA3$^+$ cells but not RORγT$^+$ cells

The reciprocal dynamic between Tregs and Tconvs expressing the same TFs raises questions about the ontogeny and stability of Tregs that express T-bet or RORγT following STM infection. Helios expression has been proposed to differentiate thymic Tregs (tTregs) from peripherally induced Tregs (pTregs)[31], but this is controversial as Helios expression has also been reported in pTregs[32–34]. Recent research has shown that Helios^{hi} and Helios^{lo} populations have distinct TCR repertoires and represent distinct populations[35]. To assess whether Tregs expressing Th TFs co-express Helios following STM infection, t-SNE plots were generated from colon CD4 T cells 11 days after mock- or STM-infection (Fig. 4b, c). Parameters used include CD44, FoxP3. T-bet, RORγT, GATA3, Helios, CXCR3 and CCR6.

Representative plots of total CD4 T cells (Fig. 4a, left and centre) and Tregs (Fig. 4a, right) are shown with gates colour-coded to identify different populations. Overlaying FoxP3$^+$ Tregs (red) FoxP3$^-$CD44^{hi} Tconvs (blue) and FoxP3$^-$CD44^{lo} naïve T cells (Fig. 4a, left) on t-SNE plots reveals distinct cluster of Tregs (red), Tconvs (dark blue) and naïve T cells (green), respectively (Fig. 4b, left). Following STM infection, the Treg cluster remains easily identifiable although the naïve T cell cluster is diminished, as expected (Fig. 4c, left). Next, T-bet$^+$ (light blue), RORγT$^+$ (plum), T-bet$^+$RORγT$^+$ (dark blue) and GATA3$^+$ (orange) cells were overlaid on t-SNE plots (Fig. 4, centre). This identifies Th1, Th17 and Th2 cells in the Tconv clusters, and T-bet$^+$, RORγT$^+$ and GATA3$^+$ Tregs (Fig. 4b-c, left). Following STM infection, the Th1 and T-bet$^+$RORγT$^+$ population are visibly increased and the Th2 population is almost absent (Fig. 4b-c, left).

Finally, FoxP3$^+$ Tregs were gated as Helios^{hi} (dark purple), Helios^{int} (pink) and Helios^{lo} (lilac) populations (Fig. 4a, right). Overlaying these populations on t-SNE plots reveals that Helios^{hi} Tregs overlay one lobe of the Treg cluster, while Helios$^{lo/int}$ Tregs overlay another (Fig. 4b-c, right). Comparing t-SNE plots of Th TFs with Helios, RORγT$^+$ Tregs are mainly confined to Helios$^{lo/int}$ cells. In contrast, GATA3$^+$ Tregs are primarily Helios^{hi} cells, while Tbet$^+$ Tregs include cells with a range of Helios expression levels. STM infection clearly increases the proportion of Tbet$^+$ Tregs, and the majority of these cells are Helios^{hi}. The proportion of Helios^{lo} Tregs is reduced by infection but RORγT$^+$ Tregs remain Helios$^{lo/int}$ cells (Fig. 4b-c). Therefore, while STM infection alters the proportion of different Treg populations, the co-expression of Th TFs with Helios remains stable.

The non-overlapping expression of Helios and RORγT is consistent with previous work suggesting Helios is a marker of tTregs[31] and RORγT is a marker of pTregs [22,36]. While it is not clear that Helios^{hi} Tregs are *bona fide* tTregs, data presented here suggests that Tbet^{+} and RORγT^{+} Tregs are distinct based on Helios expression. In the context of recent work demonstrating distinct TCR profile between Helios^{hi} and Helios^{lo} Tregs[31], T-bet^{+} and RORγT^{+} Tregs appear to be distinct populations instead of different states of differentiation.

Fig. 4

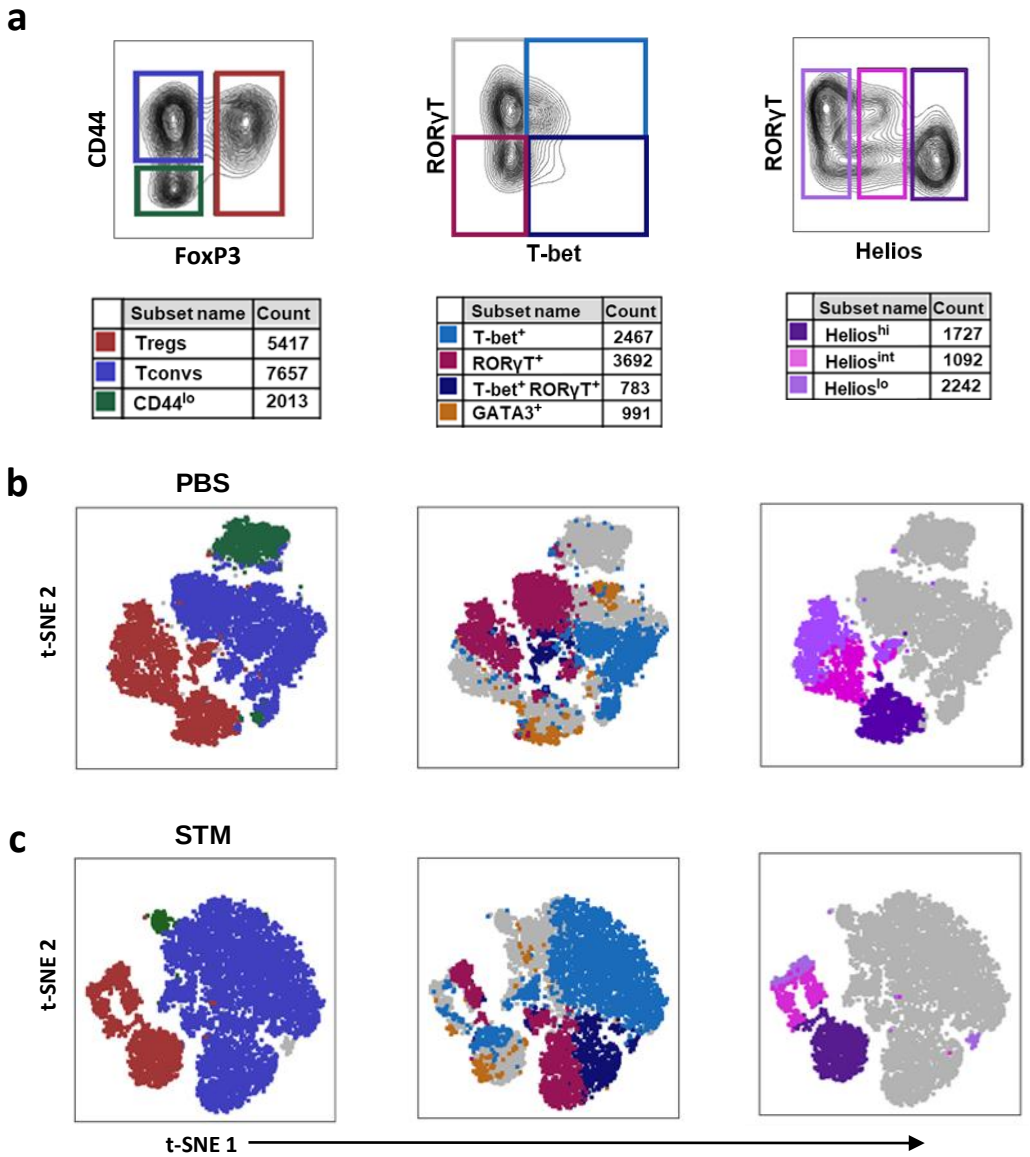

Fig. 4 Helios^{hi} Tregs can co-expressed T-bet or GATA3 but not RORγT. **a** Representative plots show gating and colour-coding of colon CD4 T cells that are FoxP3^{+} Tregs, CD44^{hi} Tconvs or FoxP3^{-}CD44^{lo} naïve T cells (left); T-bet^{+}, RORγT^{+} or T-bet^{+} RORγT^{+} Tconvs (centre); and Helios^{hi}, Helios^{int} or Helios^{lo} Tregs (right). Cell counts represent numbers of each population from 2x10^{4} CD4 T cells (gated as described in Fig. 1) and overlaid onto t-SNE plots generated using parameters of CD45, CD3, CD4, CD44, FoxP3, T-bet, RORγT, Helios, GATA3, CCR6 and CXCR3 expression. **b** t-SNE plots are shown for mock (PBS)- infected colons and **c** STM-infected colons at day 11 p.i. Grey areas are negative for all markers represented in plots shown above.

Treg depletion alters the balance of the Th1 / Th17 response following *Salmonella* infection

The reciprocal dynamic between Tregs and Tconvs during STM infection (Fig. 3) is consistent with the hypothesis that Tregs expressing Th master TFs selectively target Th subsets and skew the Th response. To determine whether Tregs are required to control the dynamic Th response to STM,

Treg depletion experiments were conducted using FoxP3^{DTR} DEREG mice, which allow ablation of FoxP3^{+} Tregs following treatment with diphtheria toxin (DT) [25]. Tregs were efficiently depleted from the peripheral blood and colon after 2 DT treatments on consecutive days. Five days post-treatment there were ~67% fewer Tregs in the blood, and ~90% fewer Tregs in the colon than in DT-treated littermate controls (Figure S6a-b).

In the first set of depletion experiments, DEREG mice were DT-treated at day 1 and 2 p.i., before being culled at day 6 p.i. (Fig. 5a). There was no significant difference in weight change between DEREG mice and wild-type (WT) littermates (Figure S6c). Treg depletion also had no significant impact on STM CFUs recovered in faeces 6 days p.i. (Figure S6d). The number of CD4^{+} T cells (Fig. 5b) and CD44^{hi} Tconvs (Fig. 5c) increased following Treg depletion, but this increase was confined to T-bet^{+} Th1 cells and T-bet^{+}RORγT^{+} cells, while the number of RORγT^{+} Th17 cells remained unchanged (Fig. 5d, left). The increased number of T-bet^{+} Tconvs underlies a decreased proportion of Th17 cells and an increased Th1 bias (Fig. 5d, left). These data demonstrate that the Th17 bias at 6 days p.i. (Fig. 2b) is dependent on Tregs, which include a higher proportion of T-bet^{+} cells at this time point (Fig. 3b).

Next, depletion experiments were conducted to determine if Tregs were also necessary to drive the Th1 bias that becomes prominent by day 11 p.i. (Fig. 2b). DT was administered day 6-7 p.i. and mice were culled at day 11 p.i. (Fig. 5e). DT treatment at this timepoint did not cause a significant difference in weight change between DEREG mice and WT littermates (Figure S6f). There was also no significant difference between faecal STM CFUs (Figure S6g), the number of total colon cells (Figure S6h), CD4 T cells (Fig. 5f) or CD44^{hi} Tconvs (Fig. 5g). Following Treg depletion, there was an increased number of both colonic Th17 and Th1 cells (Fig. 5h, left). The increase we observed in Th17 cells was greater than that of Th1 cells, reflecting a decreased Th1 bias at day 11 p.i. (Fig. 5h, right). These results demonstrate that Tregs are required for both the early Th17 and also the later Th1-biased response. In Fig. 5i, a schematic diagram depicts the Th response following STM infection and the requirement for Tregs to shape the early Th17 response and to increase the later Th1 response. The dashed-arrow is used to represent the smaller effect of RORγT^{+} Tregs in the later Th1 response, since the later Treg depletion only partially inhibits the Th1 response.

Fig. 5

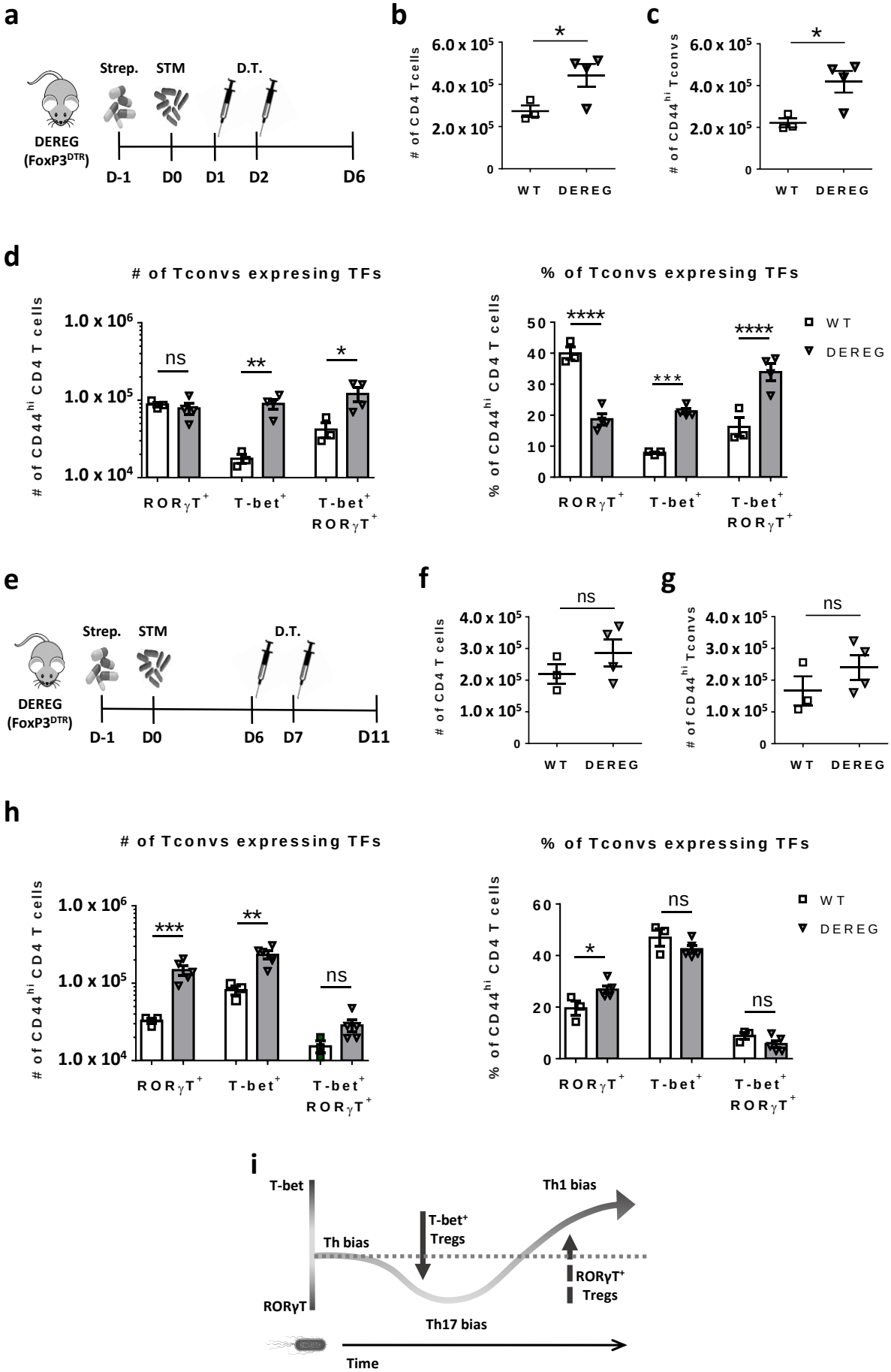
a
Strep.
STM
D.T.
DEREG
(FoxP3DTR)
D-1
D0
D1
D2
D6
b
# of CD4 Tcells
6.0 x 10^5
4.0 x 10^5
2.0 x 10^5
0
*
WT
DEREG
c
# of CD44hi Tconvs
6.0 x 10^5
4.0 x 10^5
2.0 x 10^5
0
*
WT
DEREG
d
# of Tconvs expresing TFs
# of CD44hi CD4 T cells
1.0 x 10^6
1.0 x 10^5
1.0 x 10^4
ns
**
*
RORγT+
T-bet+
T-bet+ RORγT+
% of Tconvs expresing TFs
% of CD44hi CD4 T cells
50
40
30
20
10
0
****
***
****
WT
DEREG
e
Strep.
STM
D.T.
DEREG
(FoxP3DTR)
D-1
D0
D6
D7
D11
f
# of CD4 T cells
4.0 x 10^5
3.0 x 10^5
2.0 x 10^5
1.0 x 10^5
0
ns
WT
DEREG
g
# of CD44hi Tconvs
4.0 x 10^5
3.0 x 10^5
2.0 x 10^5
1.0 x 10^5
0
ns
WT
DEREG
h
# of Tconvs expressing TFs
# of CD44hi CD4 T cells
1.0 x 10^6
1.0 x 10^5
1.0 x 10^4
***
**
ns
RORγT+
T-bet+
T-bet+ RORγT+
% of Tconvs expressing TFs
% of CD44hi CD4 T cells
60
40
20
0
*
ns
ns
WT
DEREG
i
T-bet
RORγT
Th1 bias
T-bet+ Tregs
Th bias
RORγT+ Tregs
Th17 bias
Time

Fig. 5 Treg ablation inhibits the early colonic Th17 response and later Th1 response to STM infection. **a** Experimental design for Treg depletion of streptomycin pre-treated STM-infected DEREG mice administered diphtheria toxin (D.T.) administration at day 1 and 2 p.i., with an endpoint at day 6 p.i. **b** The absolute number of colonic CD4 T cells and **c,** CD44^{hi} Tconvs in DEREG mice and wild-type (WT) littermates are shown. **d** The proportion (left) and absolute number (right) of colonic Tconvs that are RORγT^{+}, T-bet^{+} or T-bet^{+} RORγT^{+} are shown at day 6 p.i. **e** Experimental design for Treg depletion of streptomycin pre-treated STM-infected DEREG mice administered diphtheria toxin (D.T.) administration at day 6 and 7 p.i., with an endpoint at day 11 p.i. **f** The absolute number of colonic CD4 T cells and **g,** CD44^{hi} Tconvs in DEREG mice and wild-type (WT) littermates are shown. **h** The proportion (left) and absolute number (right) of colon Tconvs that are RORγT^{+} or T-bet^{+} are shown. **i** Schematic of the dynamic Th bias in colonic Tconvs following STM infection and the potential for Tregs to shape the CD4 T cell response. The baseline Th bias is indicated by a horizontal dotted line. The potential for Tregs to shape the Th bias is represented by vertical arrows, with the dashed arrow signifying a less pronounced effect of Treg depletion at the later timepoint. Data points represent individual animals (*n*=3-5) from one of three independent experiments. Means ± SEM are plotted. Statistical significance calculated by Mann-Whitney test (**b,c,f,g**) or two-way ANOVA with Holm-Šídák test (**d,h**). ns, not significant; *p<.05; **p<.01; ***p<.001; ****p<.0001.

DISCUSSION

Here we have developed an STM infection model to characterise a dynamic CD4 T cell response. In the colon we observe an early Th17 response and a later, long-lasting Th1 response. The Th1 response to STM has been shown to be important for bacterial clearance and protective immunity [5,8,9,37]. The early Th17 response described here is consistent with work identifying an early expansion and contraction of flagellin-specific Th17 cells in the intestine [38].

A dynamic and site-specific CD4 T cell response may enable the immune system to respond to changing bacterial targets, but the factors that control this response are unclear. Increasing evidence shows that Tregs expressing Th 'master' TFs can selectively suppress Th subsets and shape CD4 T cell bias [21–24,39]. To analyse the role of Tregs in controlling the Tconv response to STM, we first characterised the Treg response following infection. Results highlight a reciprocal dynamic between Tconvs and Tregs expressing T-bet or RORγT in the colon but not the cMLN (Fig. 3). The early increased proportion of colonic Th17 cells coincides with a decreased proportion of RORγT^{+} Tregs, and the later Th1 bias coincides with a decreased proportion of RORγT^{+} Tregs (Fig. 3c, d). The reciprocal dynamic between Tconvs and Tregs expressing the same TFs is consistent with the hypothesis that Th1 cells are being suppressed by T-bet^{+} Tregs and Th17 cells are being targeted by RORγT^{+} Tregs later after infection. That this dynamic occurs in the colon LP and not the cMLN suggests that reciprocity between Tconvs and Tregs is manifested in the colon itself.

Selective suppression of Th1 and Th17 cells by Tregs expressing T-bet or RORγT has been reported. Tregs have been shown to upregulate T-bet in response to type 1 inflammation and T-bet^{+} Tregs are required to control Th1-mediated inflammation [24]. In the context of *Listeria* infection, it has been shown that T-bet^{+} Tregs suppress Th1 cells and comprise a stable population that proliferates rapidly during reinfection [21]. It has also been shown that specific intestinal bacteria induce RORγT^{+}

Tregs which limit Th17-mediated colitis, and ablation of Treg-specific STAT3 induces Th17 inflammation [22,23]. Unlike previous research, here we have characterised a dynamic Th response that is reciprocal to a Treg response. This highlights the potential for Tregs to shape a multi-phase CD4 T cell response in a fine-tuned and orchestrated manner.

To demonstrate that Tregs are responsible for the changes in Th bias, we depleted Tregs at critical timepoints following infection. Day 6 p.i. was identified as a peak of the early Th17 response and day 11 p.i. was identified as a timepoint where a Th1 bias was re-established (Fig. 3d). In the first set of DEREG experiments, DT was administered at days 1 and 2 p.i. and mice were culled at day 6 p.i. Treg depletion increased the number and activation of colonic CD4 T cells (Fig. 5.2F,G), consistent with previous reports [40–43]. Treg depletion did not significantly reduce the number of STM CFUs recovered from faeces however (Fig. 5.2D), in contrast to a previous report of reduced bacterial load in DEREG animals systemically-infected with STM [44].

In the second set of depletion experiments, DT was administered days 6 and 7 p.i., and mice were culled at 11 days p.i. This time-course was selected because it maintained a 5 day period between the first DT treatment and experimental endpoint, as with the first set of DEREG experiments. It also allowed an assessment of the effect of Tregs on the Tconv response from day 6 to 11 p.i., without affecting the Tconv response before day 6 p.i. Treg depletion 6-7 days p.i. had no impact on faecal STM recovery and there was no significant increase in the number of CD4 T cells 11 days p.i., although there was a trend towards an increase in total CD4 T cells and CD44hi Tconvs (Fig. 5.4D-G). The reduced impact on cell numbers at this later time point suggests that Tregs play a less important role in constraining the number of CD4 T cells at this phase of infection. One explanation is that by 6 days p.i., Tconvs have already reached near-maximum capacity for expansion and activation. Tregs may also become less suppressive at later stages of infection, as previously reported [44].

Together, these experiments show that early Treg ablation leads to a selective increase in Th1 cells and prevents the Th17 bias at day 6 p.i. On the other hand, later Treg ablation leads to a preferential increase in the number and proportion of Th17 cells (Fig. 5d, h). As such, Tregs containing a high proportion of T-bet^{+} cells are necessary for the early Th17 response and Tregs containing an increased proportion of RORγT^{+} cells are required for an optimum Th1 bias at day 11 p.i. This indicates that the reciprocal dynamics described here are not just correlative, but that Tregs actively shape the CD4 T cell bias (Fig. 5i). These results are consistent with the hypothesis that T-bet^{+} Tregs selectively suppress the early Th1 response and shift the Tconv response towards a Th17 bias, while RORγT+ Tregs inhibit the later Th1 response.

The potential for CD4 T cells to up- or down-regulate FoxP3 expression is an alternative mechanism that could underly reciprocity between populations of Tconvs and Tregs expressing the same TFs. Plasticity between regulatory and conventional CD4 T cells has been demonstrated in several

contexts. For instance, RORγT$^+$ Tregs have been shown to downregulate FoxP3 in the absence of IL-15 and become 'ex-Tregs' that drive TH17 mediated colitis [45]. It has also been shown that Th1 cells have the potential to upregulate FoxP3 to become T-bet$^+$ Tregs [46,47]. On the other hand, evidence from lineage tracking models, transfers and *in vitro* experiments suggest that T-bet$^+$ Tregs are highly stable and retain FoxP3$^+$ expression independent of environmental conditions [21,48]. Because of the stability of T-bet$^+$ Tregs, plasticity is a less convincing explanation of reciprocity at later phases of infection. Furthermore, the distinct co-expression pattern of Helios by T-bet$^+$ and RORγT$^+$ Tregs suggests distinct ontogenies. In summary, selective suppression is a possible explanation for both reciprocal dynamics and Treg-dependent Th bias following STM infection; on the other hand, plasticity between different populations appears to be at best a partial explanation.

This research reveals a dynamic Th response in the colon after STM infection and a reciprocal dynamic between Tconvs and Tregs expressing the same TFs. Treg depletion experiments show that the early colonic Th17 response and an optimum subsequent Th1 bias are dependent on Tregs. We highlight that Tregs not only inhibit the Tconv response but shape the CD4 T cell response in a highly nuanced, site-specific and time-dependent manner. These results not only have implications for understanding how the T cell response to STM is controlled, but also for how intestinal T cell responses are balanced during infection or inflammation in general.

MATERIALS AND METHODS

Mouse strains

Male C57BL/6J mice were purchased from Envigo (Huntingdon, UK) and housed in individually ventilated cages (IVCs) prior to experimental procedures. FoxP3$^{DTR/eGFP}$ depletion of regulatory T cell (DEREG) mice were a kindly provided by Prof. Mark Travis (University of Manchester, UK) with permission from Prof. Tim Sparwasser (Medizinische Hochschule Hannover, Germany). DEREG mice were maintained and bred in IVCs. All mice were maintained under specific pathogen-free (SPF) conditions at the University of Glasgow Central Research Facility or Veterinary Research Facility (Glasgow, UK). All procedures were conducted under licenses issued by the UK Home Office under the Animals (Scientific Procedures) Act of 1986 and approved by the University of Glasgow Ethical Review Committee.

Salmonella strains and culture

STM strains SL1344-2W1S and BRD509-2W1S were kindly provided by Prof. Stephen McSorley (University of California, Davis, USA). The 2W1S strains expresses the 2W1S (EAWGALANWAVDSA) epitope in frame with OmpC[29,49]. STM cultures were streaked out on Luria-Bertani (LB) agar plates before culturing in LB broth for 5 hrs at 37°C in an incubator shaking at 180 rpm. Cultures were then back-diluted 1:10 in LB broth before static culture at 37°C overnight (O/N). Cultures were then adjusted to an OD_{600} of 1.00, centrifuged at 5,000G for 10 min, and resuspended in sterile phosphate buffered saline (PBS) at an estimated concentration of 1.0-1.5 x 10^9 CFU/ml. Following infections, actual bacterial dosage was confirmed by plating serial dilutions of STM inocula onto LB agar plates.

In vivo infections

6-10 week old mice were pre-treated with 20 mg streptomycin (Sigma-Aldrich, USA) suspended in 10 µl sterile PBS by oral gavage 24 hrs before STM infection. Mice were infected by administration of 100 µl of STM inoculum by oral gavage.

Bacterial recovery

Single cell suspensions from tissues were pelleted by centrifuging at 400 G for 5 mins and resuspended in 0.1% Triton X-100 (Sigma-Aldrich) in PBS and incubated at room temperature (RT) for 10 mins. Samples were then washed and pelleted before being resuspended in PBS, serially diluted and plated on MacConkey agar No. 2 (ThermoFisher Scientific, UK) containing 5 µg/ml streptomycin (Sigma-Aldrich) and incubated O/N at 37°C before CFUs were calculated. Bacteria were recovered from faeces and caecal contents, which were collected, aliquoted into 100 µg samples, homogenised and serially diluted and plated on MacConkey agar plates as described above.

Tissue harvest and processing

External fat, Peyer' patches (PP) and caecal patches (CP) were removed from intestinal samples and the remaining tissue was chopped and washed in HBSS with 2 mM EDTA (Gibco, UK). Samples were then incubated at 37°C shaking at 205 rpm for 10 mins, washed in EDTA buffer and the process was repeated twice. EDTA incubations and washes were repeated thrice before digestion. Digest enzyme cocktails were prepared in complete RPMI media (RPMI 1640 with 100 µg/ml streptomycin, 100 U/m penicillin, 2 mM L-Glutamine and 50 µm 2-Mercaptoethanol) with 10% FCS (all Gibco). Colon and caecal tissue were digested in an enzyme cocktail of 0.45 mg/ml collagenase V (Sigma-Aldrich), 0.65 mg/ml collagenase D (Roche, Switzerland), 1.0 mg/ml dispase (Gibco) and 30 µg/ml DNAse (Roche). Small intestines were digested with 0.5 mg/ml collagenase V (Sigma-Aldrich). Tissues were incubated at 37°C in an incubator shaking at 205 rpm for 15-20 mins. Following digests, samples were filtered through 100 µm filters, washed twice with buffer (PBS with 2% FCS and 2 mm EDTA) and filtered through a 40 µm filter.

Lymph nodes, Peyer's patches (PPs) and caecal patches (CPs) were washed in HBSS and chopped into ~1 mm pieces, passed through a 40 µm filter and suspended in buffer. Spleens were cleaned and fat was removed before passing through a 40 µm filter with FACS buffer. Samples were suspended in Ammonium-Chloride-Potassium (ACK) lysing buffer (ThermoFisher) for 3-5 mins on ice, before washing and resuspending in FACS buffer.

Staining for flow cytometry

2W1S:I-A^b tetramer was kindly provided by the NIH tetramer core facility (USA). Following infection with STM-2W1S strains, tissues were harvested and processed as described above. Samples were transferred into 96 well round bottom plates and resuspended in 25µl of tetramer mix containing complete RPMI with 10% FCS, 7 µg/ml 2W1S:IA^b tetramer, 20 µl/ml mouse serum and 10 µl/ml Fc block (CD16/32) (Biolegend, USA). Plates were incubated for 2 hrs at 37°C. Following tetramer staining, samples were stained with fixable viability dye at a 1 µl/ml in PBS. Next, antibodies for extracellular markers were prepared at 1:100 or 1:200 dilutions in FACS buffer, as specified in the list of antibodies used (Figure S7). Surface staining was performed at 4°C for 30 mins before washing and resuspension.

Transcription factor (TF) staining was carried out after cells were fixed using the eBioscience FoxP3 transcription factor staining kit (ThermoFisher) or BD Cytofix (BD Biosciences, Belgium) according to manufacturer's instructions. Cells were fixed for 1 hr at room temperature (RT) in the dark before washing and resuspending in eBioscience FoxP3 permeabilization buffer (PB) (ThermoFisher). Following fixation, TF antibodies were diluted in PB at concentrations listed in Figure S7, added to samples and incubated O/N at 4°C.

For cytokine staining, cells were treated with eBioscience cell stimulation cocktail (ThermoFisher), containing phorbol 12-myristate 13-acetate (PMA), ionomycin, brefeldin A and monensin, according to manufacturer instruction. Samples were then surface stained and fixed with BD Cytofix (BD Biosciences) according to manufacturer's instructions and stained with cytokine antibodies diluted for 2 hrs at RT. Following cytokine staining, cells were washed and resuspended in FACS buffer.

Flow cytometry

Samples were analysed using a BD LSR Fortessa analyser or sorted using a BD FACSAria IIu or III (BD Biosciences) at the Institute of Infection, Immunity and Inflammation Flow Core Facility (University of Glasgow).

Regulatory T cell depletion

Diphtheria toxin (DT) (Sigma-Aldrich) was suspended in PBS at a concentration of 10 µg/ml. DT was administered intraperitoneally (IP) twice, at a 24 hr interval, at a concentration equivalent to 30 ng/g mouse weight. DT was administered to DTR^{+} DEREG mice and DTR^{-} littermates as WT controls.

ACKNOWLEDGEMENTS

We thank Prof. Stephen McSorley for STM 2W1S strains, Profs. Mark Travis and Tim Sparwasser for DEREG mice, and the National Institute of Health Tetramer Core for 2W1S:IA^{b} tetramer. We thank Diane Vaughan and the Institute of Infection, Immunity and Inflammation Flow Core Facility for support and expertise. Thanks to Claire McIntyre, Josh Gray and Shaima Al-Khabouri for assistance with experiments. Funding was provided by the Medical Research Council (MR/1654776 and MR/N023625/1).

AUTHOR CONTRIBUTIONS

S.L.C. Conceived of study, designed experiments, conducted experiments, analysed data and prepared manuscript. S.W.F.M. and M.K.L.M Conceived of study, designed experiments, analysed data and edited manuscript. A.B.B. Conducted experiments. D.M.W. contributed to experiments involving STM infections and edited the final manuscript.

FINANCIAL SUPPORT

This work was supported by grants from the Medical Research Council (MRC/1654776/1 to S.L.C.

and MR/N023625/1 to S.W.F.M.

REFERENCES

1. Hapfelmeier, S. & Hardt, W.-D. A mouse model for S. typhimurium-induced enterocolitis. *Trends Microbiol.* **13**, 497–503 (2005).
2. Kaiser, P., Diard, M., Stecher, B. & Hardt, W.-D. The streptomycin mouse model for Salmonella diarrhea: functional analysis of the microbiota, the pathogen's virulence factors, and the host's mucosal immune response. *Immunological Reviews* **245**, 56–83 (2012).
3. Grassl, G. A., Valdez, Y., Bergstrom, K. S. B., Vallance, B. A. & Finlay, B. B. Chronic Enteric Salmonella Infection in Mice Leads to Severe and Persistent Intestinal Fibrosis. *Gastroenterology* **134**, 768-780.e2 (2008).
4. Stecher, B. *et al.* Chronic Salmonella enterica Serovar Typhimurium-Induced Colitis and Cholangitis in Streptomycin-Pretreated Nramp1+/+ Mice. *Infection and Immunity* **74**, 5047–5057 (2006).
5. Hess, J., Ladel, C., Miko, D. & Kaufmann, S. H. Salmonella typhimurium aroA- infection in gene-targeted immunodeficient mice: major role of CD4+ TCR-alpha beta cells and IFN-gamma in bacterial clearance independent of intracellular location. *J. Immunol.* **156**, 3321–3326 (1996).
6. Nauciel, C. Role of CD4+ T cells and T-independent mechanisms in acquired resistance to Salmonella typhimurium infection. *J. Immunol.* **145**, 1265–1269 (1990).
7. Kupz, A., Bedoui, S. & Strugnell, R. A. Cellular Requirements for Systemic Control of Salmonella enterica Serovar Typhimurium Infections in Mice. *Infection and Immunity* **82**, 4997–5004 (2014).
8. Pie, S., Truffa-Bachi, P., Pla, M. & Nauciel, C. Th1 response in Salmonella typhimurium-infected mice with a high or low rate of bacterial clearance. *Infect. Immun.* **65**, 4509–4514 (1997).
9. Ravindran, R. & McSorley, S. J. Tracking the dynamics of T-cell activation in response to Salmonella infection. *Immunology* **114**, 450–458 (2005).
10. Godinez, I., Keestra, A. M., Spees, A. & Bäumler, A. J. The IL-23 axis in Salmonella gastroenteritis: The IL-23 axis in Salmonella gastroenteritis. *Cellular Microbiology* **13**, 1639–1647 (2011).
11. Mayuzumi, H., Inagaki-Ohara, K., Uyttenhove, C., Okamoto, Y. & Matsuzaki, G. Interleukin-17A is required to suppress invasion of Salmonella enterica serovar Typhimurium to enteric mucosa: Importance of IL-17A in innate mucosal responses. *Immunology* **131**, 377–385 (2010).
12. Raffatellu, M. *et al.* Simian immunodeficiency virus–induced mucosal interleukin-17 deficiency promotes Salmonella dissemination from the gut. *Nature Medicine* **14**, 421–428 (2008).
13. Belkaid, Y. Regulatory T cells and infection: a dangerous necessity. *Nature Reviews Immunology* **7**, 875–888 (2007).
14. Boer, M. C., Joosten, S. A. & Ottenhoff, T. H. M. Regulatory T-Cells at the Interface between Human Host and Pathogens in Infectious Diseases and Vaccination. *Frontiers in Immunology* **6**, 2017 (2015).
15. Maizels, R. M. & Smith, K. A. Regulatory T Cells in Infection. In *Advances in Immunology* **112**, 73–136 (Elsevier, 2011).

16. Izcue, A., Coombes, J. L. & Powrie, F. Regulatory Lymphocytes and Intestinal Inflammation. *Annu. Rev. Immunol.* **27**, 313–338 (2009).
17. Cebula, A. *et al.* Thymus-derived regulatory T cells contribute to tolerance to commensal microbiota. *Nature* **497**, 258–262 (2013).
18. Yadav, M., Stephan, S. & Bluestone, J. A. Peripherally Induced Tregs – Role in Immune Homeostasis and Autoimmunity. *Frontiers in Immunology* **4**, 232 (2013).
19. Duhen, T., Duhen, R., Lanzavecchia, A., Sallusto, F. & Campbell, D. J. Functionally distinct subsets of human FOXP3+ Treg cells that phenotypically mirror effector Th cells. *Blood* **119**, 4430–4440 (2012).
20. Halim, L. *et al.* An Atlas of Human Regulatory T Helper-like Cells Reveals Features of Th2-like Tregs that Support a Tumorigenic Environment. *Cell Reports* **20**, 757–770 (2017).
21. Levine, A. G. *et al.* Stability and function of regulatory T cells expressing the transcription factor T-bet. *Nature* **546**, 421–425 (2017).
22. Sefik, E. *et al.* Individual intestinal symbionts induce a distinct population of RORγT+ regulatory T cells. *Science* **349**, 993–997 (2015).
23. Chaudhry, A. *et al.* CD4+ Regulatory T Cells Control TH17 Responses in a Stat3-Dependent Manner. *Science* **326**, 986–991 (2009).
24. Koch, M. A. *et al.* The transcription factor T-bet controls regulatory T cell homeostasis and function during type 1 inflammation. *Nature Immunology* **10**, 595–602 (2009).
25. Lahl, K. *et al.* Selective depletion of Foxp3 $^{+}$ regulatory T cells induces a scurfy-like disease. *The Journal of Experimental Medicine* **204**, 57–63 (2007).
26. Houston, S. A. *et al.* The lymph nodes draining the small intestine and colon are anatomically separate and immunologically distinct. *Mucosal Immunology* **9**, 468–478 (2016).
27. Esterházy, D. *et al.* Compartmentalized gut lymph node drainage dictates adaptive immune responses. *Nature* **569**, 126–130 (2019).
28. Zhu, J., Yamane, H. & Paul, W. E. Differentiation of Effector CD4 T Cell Populations. *Annu. Rev. Immunol.* **28**, 445–489 (2010).
29. Nelson, R. W., McLachlan, J. B., Kurtz, J. R. & Jenkins, M. K. CD4+ T cell persistence and function after infection are maintained by low-level peptide:MHC class II presentation. *J. Immunol.* **190**, 2828–2834 (2013).
30. Pham, O. H. *et al.* T cell expression of IL-18R and DR3 is essential for non-cognate stimulation of Th1 cells and optimal clearance of intracellular bacteria. *PLOS Pathogens* **13**, e1006566 (2017).
31. Thornton, A. M. *et al.* Expression of Helios, an Ikaros Transcription Factor Family Member, Differentiates Thymic-Derived from Peripherally Induced Foxp3+ T Regulatory Cells. *The Journal of Immunology* **184**, 3433–3441 (2010).
32. Akimova, T., Beier, U. H., Wang, L., Levine, M. H. & Hancock, W. W. Helios Expression Is a Marker of T Cell Activation and Proliferation. *PLoS ONE* **6**, e24226 (2011).
33. Kim, H.-J. *et al.* Stable inhibitory activity of regulatory T cells requires the transcription factor Helios. *Science* **350**, 334–339 (2015).

34. Szurek, E. *et al.* Differences in Expression Level of Helios and Neuropilin-1 Do Not Distinguish Thymus-Derived from Extrathymically-Induced CD4+Foxp3+ Regulatory T Cells. *PLOS ONE* **10**, e0141161 (2015).
35. Thornton, A. M. *et al.* Helios+ and Helios- Treg subpopulations are phenotypically and functionally distinct and express dissimilar TCR repertoires. *Eur. J. Immunol.* **49**, 398–412 (2019).
36. Park, J.-H. & Eberl, G. Type 3 regulatory T cells at the interface of symbiosis. *Journal of Microbiology* **56**, 163–171 (2018).
37. Kupz, A. *et al.* NLRC4 inflammasomes in dendritic cells regulate noncognate effector function by memory $CD8^+$ T cells. *Nat. Immunol.* **13**, 162–169 (2012).
38. Lee, S.-J. *et al.* Temporal Expression of Bacterial Proteins Instructs Host CD4 T Cell Expansion and Th17 Development. *PLoS Pathogens* **8**, e1002499 (2012).
39. Wing, J. B. & Sakaguchi, S. Multiple treg suppressive modules and their adaptability. *Frontiers in Immunology* **3**, 178 (2012).
40. Boehm, F. *et al.* Deletion of Foxp3+ regulatory T cells in genetically targeted mice supports development of intestinal inflammation. *BMC Gastroenterology* **12**, 97 (2012).
41. Kim, J. *et al.* Cutting Edge: Depletion of Foxp3+ Cells Leads to Induction of Autoimmunity by Specific Ablation of Regulatory T Cells in Genetically Targeted Mice. *The Journal of Immunology* **183**, 7631–7634 (2009).
42. Kim, J. M., Rasmussen, J. P. & Rudensky, A. Y. Regulatory T cells prevent catastrophic autoimmunity throughout the lifespan of mice. *Nature Immunology* **8**, 191–197 (2007).
43. Nyström, S. N. *et al.* Transient Treg-cell depletion in adult mice results in persistent self-reactive $CD4^+$ T-cell responses. *European Journal of Immunology* **44**, 3621–3631 (2014).
44. Johanns, T. M., Ertelt, J. M., Rowe, J. H. & Way, S. S. Regulatory T Cell Suppressive Potency Dictates the Balance between Bacterial Proliferation and Clearance during Persistent Salmonella Infection. *PLoS Pathogens* **6**, e1001043 (2010).
45. Tosiek, M. J., Fiette, L., El Daker, S., Eberl, G. & Freitas, A. A. IL-15-dependent balance between Foxp3 and RORγt expression impacts inflammatory bowel disease. *Nature Communications* **7**, 10888 (2016).
46. Amarnath, S. *et al.* The PDL1-PD1 Axis Converts Human TH1 Cells into Regulatory T Cells. *Science Translational Medicine* **3**, 111ra120-111ra120 (2011).
47. Stathopoulou, C. *et al.* PD-1 Inhibitory Receptor Downregulates Asparaginyl Endopeptidase and Maintains Foxp3 Transcription Factor Stability in Induced Regulatory T Cells. *Immunity* **49**, 247-263.e7 (2018).
48. Daniel, V., Trojan, K., Adamek, M. & Opelz, G. IFNγ+ Treg in-vivo and in-vitro represent both activated nTreg and peripherally induced aTreg and remain phenotypically stable in-vitro after removal of the stimulus. *BMC Immunology* **16**, 45 (2015).
49. Mooney, J. P. *et al.* Transient Loss of Protection Afforded by a Live Attenuated Non-typhoidal Salmonella Vaccine in Mice Co-infected with Malaria. *PLOS Neglected Tropical Diseases* **9**, e0004027 (2015).